High Resolution Neurovascular Imaging at 7T: Arterial Spin Labeling Perfusion, 4-dimensional MR Angiography and Black blood MRI

Xingfeng Shao, PhD[1], **Lirong Yan, PhD**[1,2], **Samantha Ma, PhD**[1,3], **Kai Wang, BS**[1], **Danny JJ Wang, PhD, MSCE**[1,2]

[1]Laboratory of FMRI Technology (LOFT), USC Mark & Mary Stevens Neuroimaging and Informatics Institute, Keck School of Medicine, University of Southern California, Los Angeles, CA, USA

[2]Department of Neurology, Keck School of Medicine, University of Southern California, Los Angeles, CA, USA

[3]Siemens Healthcare, Los Angeles, CA, USA

Synopsis:

Ultrahigh field (UHF) offers increased resolution and contrast for neurovascular imaging. Arterial spin labeling (ASL) methods benefit from an increased intrinsic SNR of MRI signal as well as a prolonged tracer half-life (blood T1) at UHF, allowing the visualization of layer dependent microvascular perfusion. ASL based time-resolved 4-Dimensional MR angiography (4D MRA) at 7T provides detailed depiction of both the vascular architecture and dynamic blood flow pattern with both high spatial and temporal resolutions. In addition, high resolution black blood MRI at 7T allows detailed characterization of small perforating arteries such as lenticulostriate arteries. All techniques benefit from advances in parallel RF transmission (pTx) technologies at UHF.

Corresponding contact: Danny JJ Wang, PhD, MSCE, Laboratory of FMRI Technology (LOFT), Mark & Mary Stevens Neuroimaging and Informatics Institute, Keck School of Medicine, University of Southern California (USC), jwang71@gmail.com, Phone: +1 (323) 442-7246.

Introduction

Neurovascular imaging at ultrahigh field (UHF) benefits from a high intrinsic signal to noise ratio (SNR) which can be leveraged to yield higher spatial resolution and/or higher contrast to noise ratio (CNR).[1,2] The ability to visualize fine vasculature <1mm in diameter on clinical standard (1.5T) and high-field (3T) MRI is usually limited, while UHF (7T or greater) MRI enables the evaluation of cerebrovascular lesions and vasculature in the neocortex on a submillimeter scale. UHF MRI is particularly beneficial to non-contrast enhanced MR angiography (MRA) and arterial spin labeling (ASL) perfusion with the prolonged T1 of arterial blood at higher field strength. Black blood imaging techniques also benefit from UHF with the ability to achieve isotropic submillimeter resolution, allowing the depiction of smaller perforating arteries which are critical to characterizing cerebrovascular disease, such as cerebral vasculitis and CADASIL.[3–6] Thus, the advent of 7T has resulted in a wave of research during the past decade exploring new developments in cerebrovascular imaging, which are now increasingly finding their way into clinical practice.

High resolution neurovascular imaging is also important to understanding brain function and vasculature in cortical layers. The pial arteries distribute blood from larger cerebral arteries to descending arterioles and feed capillaries in different cortical layers. After blood passes the capillary space it is collected by ascending venules and returns to pial veins towards the cortical surface.[7] Blood oxygen level dependent (BOLD) fMRI can achieve sub-millimeter spatial resolution for studying human brain function at the level of cortical layers and columns at UHF[8–10]. However, the BOLD signal is the result of complex interplays between cerebral blood flow (CBF), cerebral blood volume (CBV), and oxygen metabolism, resulting in limited fidelity for inferring the underlying neuronal activation. In addition, the BOLD signal is susceptible to venous contaminations such as the pial veins on the cortical surface that confounds laminar/columnar fMRI [9,11–13]. High resolution neurovascular imaging, such as ASL perfusion, is less affected by pial vessels, and thus is crucial to understanding the neurovascular coupling between neuronal activity and ensuing hemodynamic responses.[14]

High-resolution non-contrast enhanced MRA at UHF enables the precise depiction of cerebral vasculature including both large and small arteries, even arterioles. Time of flight (TOF) has been recognized as a mainstay for evaluating intracranial arteries. With increased intrinsic SNR and prolonged T1 at UHF, submillimeter resolution TOF (<500um) at 7T has been demonstrated[15,16] with superior angiographic contrast as a result of stronger suppression of stationary background tissue. Recently developed ASL based time-resolved 4-dimensional (4D) MRA[17,18] is another bright blood MRA technique, which allows for adequate depiction of both vascular structure and dynamic flow patterns. UHF provides sufficient SNR for 4D MRA, which could further benefit the characterization of dynamic flow patterns in cerebrovascular disorders, such as arteriovenous malformation (AVM).[17,19] High-resolution black blood MRI was originally developed for imaging extracranial (carotid bifurcation), intracranial vessel arterial wall lesions including atherosclerotic plaques and intracranial arterial stenosis.[20–22] The increased SNR at 7T leads to an overall better visualization of cerebral small vessels such as lenticulostriate arteries and potentially illustrates the effects of aging and/or vascular risk factors such as hypertension, hyperlipidemia and diabetes on the vessel structures.[23]

In this chapter, we focus on the technical developments and emerging clinical/ neuroscientific applications of ASL perfusion, 4D MRA, and T1 weighted black blood MRI at UHF. Experience with parallel RF transmission (pTx) technologies at 7T, which benefit all the above techniques, is also presented. Limitations and challenges such as specific absorption rate (SAR) and field inhomogeneity will also be discussed.

A short overview of parallel RF transmission technology at 7T

One key technical advance allowing high resolution neurovascular imaging at UHF is pTx. Currently, the conventional homogeneous bird-cage type coil driven by a single RF-pulse waveform, also known as single RF transmission (1Tx), does not possess spatial degrees of freedom and works best for uniform excitations. While usable at 3T or lower field strengths, non-uniformities arise when the wavelength of the RF waveform approaches the dimensions of the human head. Such effects are observed when imaging at UHF and result in destructive excitation field interference or shading with a characteristic strong center brightening. To mitigate these B1 inhomogeneities, pTx has been proposed as an effective solution. The most common approach for pTx is static RF shimming,[24] where all the transmit channels emit identical RF waveforms with scaled amplitudes and shifted phases. Since pTx enables more spatial degrees of freedom, tailored RF pulses or shape-specific B1 shimming can be implemented to achieve a more uniform B1 field.[25,26]

The latest 7T MAGNETOM Terra system (Siemens Healthineers, Erlangen, Germany) with the 8-channel pTx system and 8Tx/32Rx head coil (Nova Medical, Inc., Wilmington, MA, USA) offers three static B1 shim modes to correct B1 inhomogeneities including TrueForm, Patient-specific, and Volume-selective shimming. The TrueForm shim mode uses 45° phase increments for each adjacent transmit channel to mimic the 1Tx circularly polarized (CP) coil. Due to the increased spatial coverage with the pTx coil geometry, TrueForm shimming with the pTx system can already achieve improved RF uniformity in the temporal and subcortical brain regions compared to 1Tx. In Patient-specific shim mode, the RF excitation is parameterized relative to the B1 maps of the registered subject. This method is optimized for B1 shimming of the whole volume specified by the slice group. Lastly, Volume-selective shim mode optimizes the B1 field to a specific volume chosen by the user, which is often helpful for improving the homogeneity in an anatomically specific region of interest.[27] Compared to acquisition with 1Tx, the use of pTx significantly improves the RF uniformity across the brain tissue (Figure 1 (A)), leading to higher SNR in the temporal and subcortical regions (Figure 1 (B)) and ultimately supporting high resolution imaging across the whole brain at UHF.

Arterial Spin Labeled perfusion at 7T

CBF or perfusion measured by ASL is a key parameter for *in vivo* assessment of neurovascular function. ASL signal is close to the site of neural activation as most of the labeled arterial water exchanges with tissue water in capillaries.[28] It has been shown that ASL perfusion fMRI is able to visualize orientation columns in the cat visual cortex with superior spatial resolution compared to BOLD fMRI.[29] The hemodynamic response of perfusion signals has also been shown to arise ~1sec earlier than that of BOLD signals.[30]

Unlike BOLD fMRI that detects relative signal changes between two conditions, ASL provides quantitative perfusion measurements both at rest and during task activation. UHF ASL has the dual benefits of increased SNR that scales with B0 field and prolonged tracer half-life (blood T1),[31] therefore it may overcome the major limitation of ASL in terms of low SNR. Figure 2 (A) shows more than 3-fold SNR gain for 7T ASL compared to 3T ASL predicted by theory. Indeed, our experimental data using turbo-FLASH based ASL at 7T demonstrated the feasibility of perfusion imaging with near sub-millimeter spatial resolution which is not feasible at 3T (Fig. 2B).[32]

In order to achieve whole-brain high resolution perfusion imaging at 7T, we have recently taken advantage of the 8Tx/32Rx head coil with TrueForm B1 shimming mode on the 7T Terra system, which allowed the application of pseudo-continuous ASL (pCASL) at the base of the brain.[33] In addition, a novel time-dependent 2D-CAIPIRINHA (controlled aliasing in parallel imaging results in higher acceleration) technique[34] was implemented in a 3D Gradient and Spin Echo (GRASE) sequence to achieve robust high resolution and highly accelerated 3D imaging (up to 12-fold) by efficiently exploiting coil sensitivity variations along both phase and slice dimensions (lower coil g-factor), as well as temporal incoherence of sampling patterns across ASL measurements (Fig. 3 (A)).[33] A novel image reconstruction method employing both spatial and temporal total-generalized-variation (TGV) regularization[35] was applied to reconstruct high resolution (2 mm isotropic) CBF maps with nearly whole brain coverage and 12-fold acceleration (Fig. 3 (B)). This novel ASL-TGV method also had denoising capabilities to minimize effects of head motion and physiological noise on perfusion images at 7T.

Adiabatic pulses have been commonly used as the inversion pulse for pulsed ASL (PASL) to address the issues of B0 and B1 inhomogeneity at UHF. To improve the quality and accuracy of the perfusion map acquired at 7T, we recently optimized and systematically evaluated four commonly used adiabatic inversion pulses including the Hyperbolic Secant (HS) pulse,[36] Wideband Uniform Rate Smooth Truncation (WURST) pulse,[37] Frequency Offset Correction Inversion (FOCI) pulse,[38] and time-resampled FOCI (trFOCI) pulse[39] based on a custom-defined loss function that took into account the labeling efficiency and the residual tissue signal.[40] This study again utilized the 8Tx/32Rx head coil with TrueForm B1 shimming mode on 7T Terra. The perfusion maps of the 4 pulse sequences of one representative subject are shown in Figure 4. The optimized WURST pulse achieved a good balance between high labeling efficiency and low residual tissue signal, with higher labeling efficiency than HS and trFOCI pulses, and lower residual tissue signal than FOCI pulse. The relative labeling efficiency versus residual tissue signal of the WURST PASL sequence was significantly higher than any of the other three sequences (P<0.01 for each case). Furthermore, the PASL sequence with the optimized WURST pulse was able to provide nearly whole brain perfusion imaging at 7T.

Layer Dependent Perfusion Imaging

Because the thickness of the cerebral cortex is usually less than 3 mm,[41] sub-millimeter spatial resolution is required to study layer or depth dependent structural and/or physiological changes. Recent research has demonstrated that the pCASL labeling scheme

combined with efficient 3D inner-volume GRASE readout and background suppression has the capability of revealing layer dependent CBF at UHF of 7T.[14] Since the ASL signal is quantitative and originated primarily from capillaries and brain tissue, this new development opens the door to investigating neurovascular coupling with an unprecedented precision at the laminar level.

Figure 5 shows sub-millimeter multi-delay perfusion images (B) and a CBF map (C) acquired from one healthy subject (Female, 38 years old) using pCASL with background suppressed 3D inner-volume GRASE at 7T. The labeling plane was applied above the circle of Willis and 50 mm below the center of the imaging volume (left motor cortex) using the 1Tx/32Rx coil. The in-plane resolution was 0.5 mm after interpolation, and slice thickness was 1.4 mm. Three layers of gray matter (superficial, middle, deep) were manually segmented based on co-registered T1w MPRAGE images. Figure 5 (D) and (E) show the bar-plot of multi-delay perfusion signals and CBF values averaged from four subjects (2 male and 2 female, 31.5±3.1 years old). Perfusion signal was significantly higher in the middle layer than the superficial or deep layer (~20%) at PLD = 1000 ms and 1500 ms (P<0.05). Average CBF was 42.1, 49.4, and 40.3 ml/100g/min in the superficial, middle, and deep layers, respectively. CBF was significantly higher in the middle layer (~20%, P<0.001), which matches well with the highest capillary density observed in the middle layers as reported in anatomical studies in animals and specimens of human brain tissue.[42] The capability of imaging CBF in cortical layers allows new opportunities for investigating the microvascular blood supply and neurovascular coupling in a laminar fashion.

4-dimensional MR angiography at 7T

Besides tissue perfusion or CBF, ASL also offers angiographic contrast. With a shorter post-labeling delay time after ASL preparation, the majority of labeled blood is still within arteries, thus MR angiogram is obtained. Over the past decade, a number of studies have applied ASL for MRA purposes by taking advantage of recent advances in both ASL labeling and image acquisition.[17,18,43–49] In particular, an ASL-based time-resolved non-contrast enhanced 4-dimensional MRA (4D MRA) has been developed, which offers spatial resolution of approximately 1mm^3 and temporal resolution of 50~100ms.[17,44] This 4D MRA shows potential for characterizing cerebrovascular dynamic flow patterns in cerebrovascular disorders, such as AVM.[19,50,51] However, it remains a challenge to capture the draining vein, which serves as a critical criterion in clinical diagnosis in AVM,[19,50,51] when using 4D MRA at conventional 1.5T and 3T as a result of relatively short trace half-life (blood T1).

The SNR of ASL-based MRA is considerably higher than that of ASL perfusion, given the high concentration of labeled blood within an arterial voxel as well as minimal post-labeling delay time. UHF further benefits ASL-based MRA with increased intrinsic SNR and prolonged blood T1. Therefore, 4D MRA at 7T allows for detailed characterization of vascular architecture as well as dynamic flow patterns. Our previous work has initially demonstrated the feasibility of 4D MRA at 7T using both standard 3D Cartesian acquisition and advanced non-cartesian acquisition with golden-angle stack-of-stars radial sampling.[52] Figure 6 shows six selected temporal frames of 4D MRA with a spatial resolution of isotropic 1mm and temporal resolution of 96 ms collected on 7T Terra from a healthy

volunteer using the 1Tx head coil. One can appreciate the fine vascular structures as well as dynamic blood flow through the cerebral vasculature. 4D MRA at 7T also shows improved delineation of AVM features, especially the draining veins. Figure 7 shows a comparison of 4D MRA at 3T and 7T for an AVM case. We can clearly observe the labeled blood flow through the feeding arteries and nidus on both 3T and 7T, matching the DSA findings nicely. However, the draining vein can only be clearly visualized at 7T due to the prolonged blood T1, while it failed to be visible at 3T. Therefore, 7T possesses potential clinical utility (and advantage over 3T) in the evaluation of AVMs and other cerebrovascular diseases with slow flow.

Black Blood MRI at 7T

High-resolution black blood MRI is a recent technique originally developed for imaging intracranial vessel wall and plaque using 3D T1-weighted turbo spin-echo (TSE) sequences with variable flip angles (VFA).[53–55] The technique has previously been implemented on various platforms and field strengths, allowing the potential for straightforward translation to clinical imaging. Particularly at UHF, the long echo train of the TSE technique offers three advantages for visualizing small vessels: 1) adequate flow suppression by inherent dephasing of flowing signals (black blood MRI); 2) high spatial resolution (isotropic 0.5mm or higher); and 3) near whole-brain coverage in a clinically acceptable time (<10 min). In addition to providing improved plaque characterization at the large artery vessel wall,[56] these features suggest that black blood MRI is particularly suitable for visualizing cerebral small vessels such as the lenticulostriate arteries (LSAs) and other perforating arteries as well.

Our previous study demonstrated the optimization of the T1-weighted TSE-VFA sequence at UHF for the delineation of LSAs in a healthy cohort.[23] As a comparison, 7T TOF MRA is the reference standard for visualizing and quantifying LSAs.[57] As shown in Figure 8, black blood MRI whether at 3T or 7T was able to detect more LSAs likely because the saturation effect of TOF MRA on slow flowing spins led to compromised delineation of smaller LSAs usually on the medial side of the middle cerebral artery. Conversely, LSAs can be reliably visualized by T1w TSE-VFA due to combined effects of longer T1/T2 values of arterial blood and flow induced phase dispersion during TSE readout at both 3T and 7T. The delineation of LSAs in T1-weighted TSE-VFA images can be a useful tool to evaluate and potentially illustrate the effects of aging and/or vascular risk factors such as hypertension, hyperlipidemia, and diabetes on the vessel structures. This may also be a possible technique for the visualization of small hypertensive related Charcot-Bouchard aneurysms of the LSAs which can result is catastrophic basal ganglionic hemorrhages. Given the sharpness and improved SNR at UHF, automated or deep learning-based segmentation algorithms can be applied to these high-resolution black blood images in order to perform quantitative shape analysis of LSA morphology.[58]

There are still some challenges to address regarding the use of black blood MRI for clinical small vessel characterization at UHF. The image contrast of small perforating arteries may be affected by B1 inhomogeneity, especially at UHF. Fortunately, the central location of LSAs at the central "bright spot" of B1+ field due to dielectric effects at 7T is favorable for

enhancing the CNR of LSAs. However, in order to observe other perforating arteries in the neocortex or larger vessels at the base of the brain, solutions such as pTx shimming should be applied. Figure 9 demonstrates the benefit of utilizing pTx B1 shimming for improving detailed delineation of perforating arteries as well as achieving more homogeneous signal at the base of the brain near the circle of Willis. With the better coverage provided by pTx, we can take full advantage of the whole-brain, high resolution features of T1-weighted TSE-VFA for the morphological evaluation of cerebral vasculature from arteries to very small arterioles.

Potentials and Challenges of Neurovascular Imaging at 7T

In this paper, we showcase several new developments in neurovascular imaging at 7T including high resolution PASL and pCASL with near whole brain coverage, cortical layer dependent perfusion imaging, 4D time resolved MRA and black blood MRI. These new techniques have many clinical and neuroscientific applications. For instance, high resolution ASL at UHF allows the characterization of small cortical lesions in multiple sclerosis that previously could only be imaged using contrast enhanced MRI.[59] The increased SNR and prolonged blood T1 (>2 sec) at UHF should make it feasible for reliable measurement of white matter perfusion using ASL, which has been challenging due to the increased transit time and lower CBF in white matter than in gray matter.[60] The capability for laminar perfusion imaging in human brain is groundbreaking. To date, such information can only be obtained by anatomical studies in animals and specimens of human brain tissue.[42] The laminar profile of resting perfusion may be treated as a surrogate index of microvascular density across the human cortex, as well as its variations with neurodegeneration in Alzheimer's disease and multiple sclerosis. Such information can be incorporated into modeling work to explain depth dependent BOLD responses.[9] In addition, task activation induced perfusion changes can be investigated in a layer dependent fashion without the contamination of pial veins seen in BOLD fMRI. Given the tight neurovascular coupling between neuronal activity and microvascular perfusion, our capability to infer underlying neuronal activity in health and disease will be greatly enhanced.

The increased SNR and prolonged T1 at UHF are also highly beneficial for both bright and black blood MRA/MRI. As shown in Figure 7, the draining vein of AVM can only be visualized by 4D MRA at 7T but not at 3T. Black blood MRI with T1w TSE-VFA at both 3T and 7T is able to visualize more LSAs than 7T TOF MRA at 7T, and offers concurrent evaluation of vessel wall and parenchymal lesions. Black blood MRI at 7T provides sharper delineation of LSAs than 3T, especially in the distal portions of the vessels (Fig. 8). However, perivascular space (PVS) also appears dark in T1w TSE-VFA images, and the spatial resolution of existing black blood MRI does not allow differentiation of lumen from PVS signals of small vessels. It will be interesting to combine both bright and black blood MRA/MRI to fully characterize the morphology and function of small vessels in human brain at UHF. Such capability will be highly appealing for the characterization of cerebral small vessel disease (cSVD) which is a major cause of stroke and dementia.[61]

The challenges of neurovascular imaging at UHF include B1/B0 field inhomogeneities and SAR constraints. The pTx technology already showed promise in mitigating B1 field

inhomogeneity in our 7T studies, although we only used the basic TrueForm shim mode that simulates 1Tx excitation. For the next step, we will compare TrueForm with "Patient-specific" and "Volume-selective" shimming modes, and the latter two are expected to yield a more homogeneous B1 field at the cost of a greater level of SAR. For adiabatic inversion pulses, the minimum B1 intensity can be maximized using RF shimming to improve the labeling efficiency.[62] More advanced strategies such as dynamic pTx pulses[63] can be further applied, where each RF channel plays out channel-specific waveforms creating time-dependent spatial interference patterns to reach an ideal tradeoff between B1 field homogeneity and SAR.

In summary, we present several new developments for high-resolution neurovascular imaging at 7T. In conjunction with other technical advances at UHF such as pTx technologies, the suite of new methods can characterize the structure and function of the cerebral vasculature from arteries to arterioles and capillaries with sub-millimeter spatial resolution.

Acknowledgement:

References:

1. De Cocker LJ, Lindenholz A, Zwanenburg JJ, et al. Clinical vascular imaging in the brain at 7 T. Neuroimage. 2018;168:452–458. [PubMed: 27867089]

2. Rutland J, Delman B, Gill C, Zhu C, Shrivastava R, Balchandani P. Emerging Use of Ultra-High-Field 7T MRI in the Study of Intracranial Vascularity: State of the Field and Future Directions. American Journal of Neuroradiology. 2020;41(1):2–9. [PubMed: 31879330]

3. Bousser MG, Biousse V. Small vessel vasculopathies affecting the central nervous system. J Neuroophthalmol. 2004;24(1):56–61. [PubMed: 15206441]

4. Pantoni L Cerebral small vessel disease: from pathogenesis and clinical characteristics to therapeutic challenges. Lancet Neurol. 2010;9(7):689–701. [PubMed: 20610345]

5. Pantoni L, Pescini F, Nannucci S, et al. Comparison of clinical, familial, and MRI features of CADASIL and NOTCH3-negative patients. Neurology. 2010;74(1):57–63. [PubMed: 20038773]

6. Scolding NJ. Central nervous system vasculitis. Semin Immunopathol. 2009;31(4):527–536. [PubMed: 19908043]

7. Schmid F, Barrett MJP, Jenny P, Weber B. Vascular density and distribution in neocortex. Neuroimage. 2019;197:792–805. [PubMed: 28669910]

8. Koopmans PJ, Barth M, Orzada S, Norris DG. Multi-echo fMRI of the cortical laminae in humans at 7 T. Neuroimage. 2011;56(3):1276–1285. [PubMed: 21338697]

9. Polimeni JR, Fischl B, Greve DN, Wald LL. Laminar analysis of 7 T BOLD using an imposed spatial activation pattern in human V1. Neuroimage. 2010;52(4):1334–1346. [PubMed: 20460157]

10. Cheng K, Waggoner RA, Tanaka K. Human ocular dominance columns as revealed by high-field functional magnetic resonance imaging. Neuron. 2001;32(2):359–374. [PubMed: 11684004]

11. De Martino F, Zimmermann J, Muckli L, Ugurbil K, Yacoub E, Goebel R. Cortical depth dependent functional responses in humans at 7T: improved specificity with 3D GRASE. PloS one. 2013;8(3).

12. Yacoub E, Shmuel A, Logothetis N, U urbil K. Robust detection of ocular dominance columns in humans using Hahn Spin Echo BOLD functional MRI at 7 Tesla. Neuroimage. 2007;37(4):1161–1177. [PubMed: 17702606]

13. Moerel M, De Martino F, Kemper VG, et al. Sensitivity and specificity considerations for fMRI encoding, decoding, and mapping of auditory cortex at ultra-high field. Neuroimage. 2018;164:18–31. [PubMed: 28373123]

14. Shao X, Wang K, Wang DJ. 7T high-resolution arterial spin labeling reveals layer dependent cerebral blood flow. In. Vol 27 Proc ISMRM 20192019.

15. Kang CK, Park CW, Han JY, et al. Imaging and analysis of lenticulostriate arteries using 7.0-Tesla magnetic resonance angiography. Magn Reson Med. 2009;61(1):136–144. [PubMed: 19097221]

16. Zwanenburg JJ, Hendrikse J, Takahara T, Visser F, Luijten PR. MR angiography of the cerebral perforating arteries with magnetization prepared anatomical reference at 7T: Comparison with time-of-flight. Journal of Magnetic Resonance Imaging: An Official Journal of the International Society for Magnetic Resonance in Medicine. 2008;28(6):1519–1526.

17. Yan L, Wang S, Zhuo Y, et al. Unenhanced dynamic MR angiography: high spatial and temporal resolution by using true FISP–based spin tagging with alternating radiofrequency. Radiology. 2010;256(1):270–279. [PubMed: 20574100]

18. Yan L, Salamon N, Wang DJ. Time-resolved noncontrast enhanced 4-D dynamic magnetic resonance angiography using multibolus TrueFISP-based spin tagging with alternating radiofrequency (TrueSTAR). Magn Reson Med. 2014;71(2):551–560. [PubMed: 23440649]

19. Yu S, Yan L, Yao Y, et al. Noncontrast dynamic MRA in intracranial arteriovenous malformation (AVM): comparison with time of flight (TOF) and digital subtraction angiography (DSA). Magnetic resonance imaging. 2012;30(6):869–877. [PubMed: 22521994]

20. Zhu C, Haraldsson H, Tian B, et al. High resolution imaging of the intracranial vessel wall at 3 and 7 T using 3D fast spin echo MRI. Magnetic Resonance Materials in Physics, Biology and Medicine. 2016;29(3):559–570.

21. Harteveld AA, van der Kolk AG, van der Worp HB, et al. High-resolution intracranial vessel wall MRI in an elderly asymptomatic population: comparison of 3T and 7T. European radiology. 2017;27(4):1585–1595. [PubMed: 27387876]

22. Baradaran H, Patel P, Gialdini G, et al. Quantifying intracranial internal carotid artery stenosis on MR Angiography. American Journal of Neuroradiology. 2017;38(5):986–990. [PubMed: 28302605]

23. Ma SJ, Sarabi MS, Yan L, et al. Characterization of lenticulostriate arteries with high resolution black-blood T1-weighted turbo spin echo with variable flip angles at 3 and 7 Tesla. Neuroimage. 2019;199:184–193. [PubMed: 31158475]

24. Zhu Y Parallel excitation with an array of transmit coils. Magn Reson Med. 2004;51(4):775–784. [PubMed: 15065251]

25. Hoult DI, Phil D. Sensitivity and power deposition in a high-field imaging experiment. J Magn Reson Imaging. 2000;12(1):46–67. [PubMed: 10931564]

26. Ibrahim TS, Lee R, Baertlein BA, Kangarlu A, Robitaille PL. Application of finite difference time domain method for the design of birdcage RF head coils using multi-port excitations. Magn Reson Imaging. 2000;18(6):733–742. [PubMed: 10930783]

27. TimTX syngo MR E12 Operator Manual. In. Erlangen, Germany: Siemens Healthcare GmbH; 2018.

28. Detre JA, Wang J. Technical aspects and utility of fMRI using BOLD and ASL. Clinical Neurophysiology. 2002;113(5):621–634. [PubMed: 11976042]

29. Duong TQ, Kim D-S, U̇rbil K, Kim S-G. Localized cerebral blood flow response at submillimeter columnar resolution. Proceedings of the National Academy of Sciences. 2001;98(19):10904–10909.

30. Liu HL, Pu Y, Nickerson LD, Liu Y, Fox PT, Gao JH. Comparison of the temporal response in perfusion and BOLD-based event-related functional MRI. Magnetic Resonance in Medicine: An Official Journal of the International Society for Magnetic Resonance in Medicine. 2000;43(5):768–772.

31. Wang J, Alsop DC, Li L, et al. Comparison of quantitative perfusion imaging using arterial spin labeling at 1.5 and 4.0 Tesla. Magnetic Resonance in Medicine: An Official Journal of the International Society for Magnetic Resonance in Medicine. 2002;48(2):242–254.

32. Zuo Z, Wang R, Zhuo Y, Xue R, Lawrence KSS, Wang DJ. Turbo-FLASH based arterial spin labeled perfusion MRI at 7 T. PloS one. 2013;8(6).

33. Shao X, Spann SM, Wang K, Yan L, Rudolf S, Wang DJ. High-resolution whole brain ASL perfusion imaging at 7T with 12-fold acceleration and spatial-temporal regularized reconstruction. In. Vol 28 Proc. Intl. Soc. Mag. Reson. Med2020.

34. Breuer FA, Blaimer M, Mueller MF, et al. Controlled aliasing in volumetric parallel imaging (2D CAIPIRINHA). Magnetic Resonance in Medicine: An Official Journal of the International Society for Magnetic Resonance in Medicine. 2006;55(3):549–556.

35. Spann SM, Shao X, Wang DJ, et al. Robust single-shot acquisition of high resolution whole brain ASL images by combining time-dependent 2D CAPIRINHA sampling with spatio-temporal TGV reconstruction. Neuroimage. 2020;206:116337. [PubMed: 31707191]

36. Silver M, Joseph R, Hoult D. Highly selective π2 and π pulse generation. Journal of Magnetic Resonance. 1969;59(2):347–351.

37. Kupce E Adiabatic pulses for wideband inversion and broadband decoupling. Journal of magnetic resonance. 1995;Series A(115):4.

38. Ordidge RJ, Wylezinska M, Hugg JW, Butterworth E, Franconi F. Frequency offset corrected inversion (FOCI) pulses for use in localized spectroscopy. Magn Reson Med. 1996;36(4):562–566. [PubMed: 8892208]

39. Hurley AC, Al-Radaideh A, Bai L, et al. Tailored RF pulse for magnetization inversion at ultrahigh field. Magn Reson Med. 2010;63(1):51–58. [PubMed: 19859955]

40. Wang K, Shao X, Yan L, Jin J, Wang D. Optimization of adiabatic pulses for Pulsed ASL at 7T – Comparison with Pseudo-continuous ASL In. Vol 282020.

41. Tamnes CK, Herting MM, Goddings A-L, et al. Development of the cerebral cortex across adolescence: a multisample study of inter-related longitudinal changes in cortical volume, surface area, and thickness. Journal of Neuroscience. 2017;37(12):3402–3412. [PubMed: 28242797]

42. Lauwers F, Cassot F, Lauwers-Cances V, Puwanarajah P, Duvernoy H. Morphometry of the human cerebral cortex microcirculation: general characteristics and space-related profiles. Neuroimage. 2008;39(3):936–948. [PubMed: 17997329]

43. van Osch MJ, Hendrikse J, Golay X, Bakker CJ, van der Grond J. Non-invasive visualization of collateral blood flow patterns of the circle of Willis by dynamic MR angiography. Medical image analysis. 2006;10(1):59–70. [PubMed: 15950521]

44. Bi X, Weale P, Schmitt P, Zuehlsdorff S, Jerecic R. Non-contrast-enhanced four-dimensional (4D) intracranial MR angiography: a feasibility study. Magnetic resonance in medicine. 2010;63(3):835–841. [PubMed: 20187191]

45. Okell TW, Schmitt P, Bi X, et al. Optimization of 4D vessel-selective arterial spin labeling angiography using balanced steady-state free precession and vessel-encoding. NMR in Biomedicine. 2016;29(6):776–786. [PubMed: 27074149]

46. Shao X, Zhao Z, Russin J, et al. Quantification of intracranial arterial blood flow using noncontrast enhanced 4D dynamic MR angiography. Magn Reson Med. 2019;82(1):449–459. [PubMed: 30847971]

47. Song HK, Yan L, Smith RX, et al. Noncontrast enhanced four-dimensional dynamic MRA with golden angle radial acquisition and K-space weighted image contrast (KWIC) reconstruction. Magn Reson Med. 2014;72(6):1541–1551. [PubMed: 24338944]

48. Zhou Z, Han F, Yu S, et al. Accelerated noncontrast-enhanced 4-dimensional intracranial MR angiography using golden-angle stack-of-stars trajectory and compressed sensing with magnitude subtraction. Magn Reson Med. 2018;79(2):867–878. [PubMed: 28480537]

49. Wu H, Block WF, Turski PA, Mistretta CA, Johnson KM. Noncontrast-enhanced three-dimensional (3D) intracranial MR angiography using pseudocontinuous arterial spin labeling and accelerated 3D radial acquisition. Magn Reson Med. 2013;69(3):708–715. [PubMed: 22532423]

50. Hadizadeh DR, Kukuk GM, Steck DT, et al. Noninvasive evaluation of cerebral arteriovenous malformations by 4D-MRA for preoperative planning and postoperative follow-up in 56 patients: comparison with DSA and intraoperative findings. AJNR Am J Neuroradiol. 2012;33(6):1095–1101. [PubMed: 22300925]

51. Xu J, Shi D, Chen C, et al. Noncontrast-enhanced four-dimensional MR angiography for the evaluation of cerebral arteriovenous malformation: a preliminary trial. J Magn Reson Imaging. 2011;34(5):1199–1205. [PubMed: 21769984]

52. Cong F, Zhuo Y, Yu S, et al. Noncontrast-enhanced time-resolved 4D dynamic intracranial MR angiography at 7T: A feasibility study. J Magn Reson Imaging. 2018;48(1):111–120. [PubMed: 29232026]

53. Qiao Y, Steinman DA, Qin Q, et al. Intracranial arterial wall imaging using three-dimensional high isotropic resolution black blood MRI at 3.0 Tesla. Journal of Magnetic Resonance Imaging. 2011;34(1):22–30. [PubMed: 21698704]

54. Qiao Y, Zeiler SR, Mirbagheri S, et al. Intracranial plaque enhancement in patients with cerebrovascular events on high-spatial-resolution MR images. Radiology. 2014;271(2):534–542. [PubMed: 24475850]

55. Fan Z, Yang Q, Deng Z, et al. Whole-brain intracranial vessel wall imaging at 3 T esla using cerebrospinal fluid–attenuated T1-weighted 3 D turbo spin echo. Magnetic resonance in medicine. 2017;77(3):1142–1150. [PubMed: 26923198]

56. Van Der Kolk A, Zwanenburg J, Denswil N, et al. Imaging the intracranial atherosclerotic vessel wall using 7T MRI: initial comparison with histopathology. American Journal of Neuroradiology. 2015;36(4):694–701. [PubMed: 25477359]

57. Cho ZH, Kang CK, Han JY, et al. Observation of the lenticulostriate arteries in the human brain in vivo using 7.0T MR angiography. Stroke. 2008;39(5):1604–1606. [PubMed: 18340096]

58. Ma SJ, Sarabi MS, Wang K, et al. Deep Learning Segmentation of Lenticulostriate Arteries on 3D Black Blood MRI. In. Vol 28 Proc. Intl. Soc. Mag. Reson. Med.2020.

59. Dury RJ, Falah Y, Gowland PA, Evangelou N, Bright MG, Francis ST. Ultra-high-field arterial spin labelling MRI for non-contrast assessment of cortical lesion perfusion in multiple sclerosis. Eur Radiol. 2019;29(4):2027–2033. [PubMed: 30280247]

60. Wu W-C, Lin S-C, Wang DJ, Chen K-L, Li Y-D. Measurement of cerebral white matter perfusion using pseudocontinuous arterial spin labeling 3T magnetic resonance imaging– an experimental and theoretical investigation of feasibility. PloS one. 2013;8(12).

61. Ma SJ, Jann K, Barisano G, et al. CHARACTERIZATION OF LENTICULOSTRIATE ARTERIES USING ARTERIAL SPIN LABELING AND HIGH-RESOLUTION 3D BLACK-BLOOD MRI AS AN IMAGING MARKER IN VASCULAR COGNITIVE IMPAIRMENT AND DEMENTIA. Alzheimer's & Dementia: The Journal of the Alzheimer's Association. 2019;15(7):P1103–P1104.

62. Balchandani P, Khalighi MM, Hsieh SS, Setsompop K, Pauly J, Spielman D. Adiabatic B1 Shimming Algorithm for Multiple Channel Transmit at 7T. Proc ISMRM. 2011;19:2907.

63. Katscher U, Bornert P, Leussler C, van den Brink JS. Transmit SENSE. Magn Reson Med. 2003;49(1):144–150. [PubMed: 12509830]

64. Ma SJ, Zhao C, Wang K, et al. Anatomical NeuroImaging with Single and Parallel Transmission at Ultra-high Field: A Comparison of Image Quality and User Experience. In. Vol 28 Proc. Intl. Soc. Mag. Reson. Med2020.

Key Points

1. Ultrahigh field (UHF) offers increased resolution and contrast for neurovascular imaging.

2. UHF ASL has dual benefits of increased SNR and blood T1.

3. High resolution 7T ASL allows layer dependent perfusion imaging.

4. 4D MRA at 7T provides detailed visualization of vascular architecture and dynamic blood flow pattern.

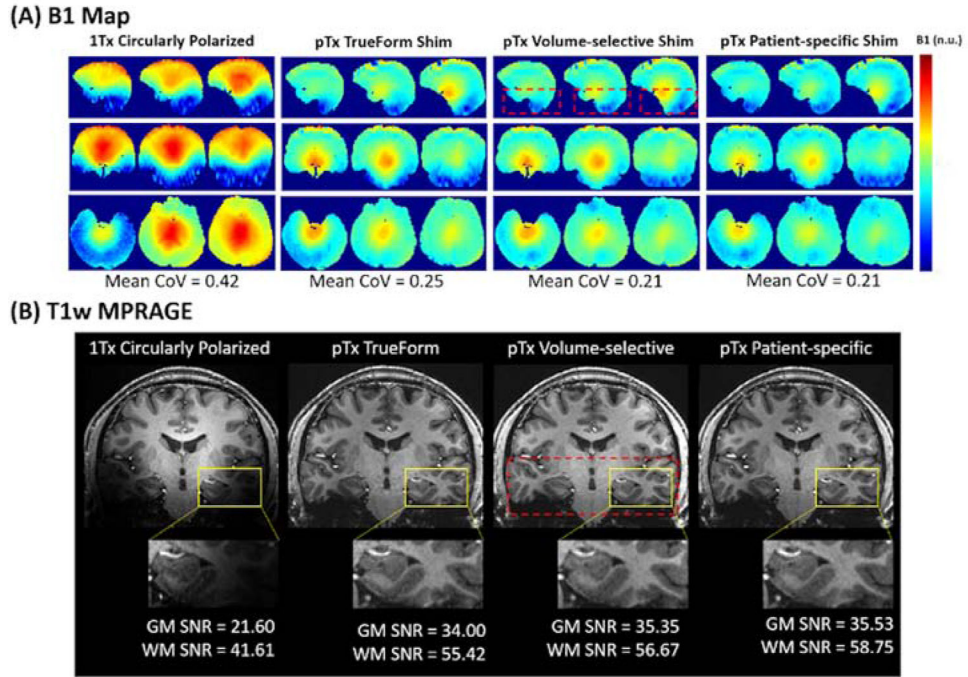5. Black blood MRI at 7T allows characterization of small perforating arteries such as lenticulostriate arteries.

Figure 1.

In vivo comparisons of various coil configurations using either pTx-mode or 1Tx-mode. (A) Measured B1+ field distributions in sagittal (top row), axial (middle row), and coronal (bottom row) views. Mean coefficient of variation (CoV = std/mean) was measured after each B1+ field shimming process. (B) Gray matter (GM) and white matter (WM) SNR comparison demonstrating the increased coverage with pTx for T1-weighted MPRAGE images. pTx Patient-specific shimming produced the highest SNR for gray-white matter contrast in the temporal lobe region (yellow box). The red dashed box indicates the volume prescribed for pTx Volume-selective B1 shimming. *Adapted from* Ma SJ, Zhao C, Wang K, et al. Anatomical NeuroImaging with Single and Parallel Transmission at Ultra-high Field: A Comparison of Image Quality and User Experience. Intl Soc Mag Reson Med. 2020;Vol 28. With permission.
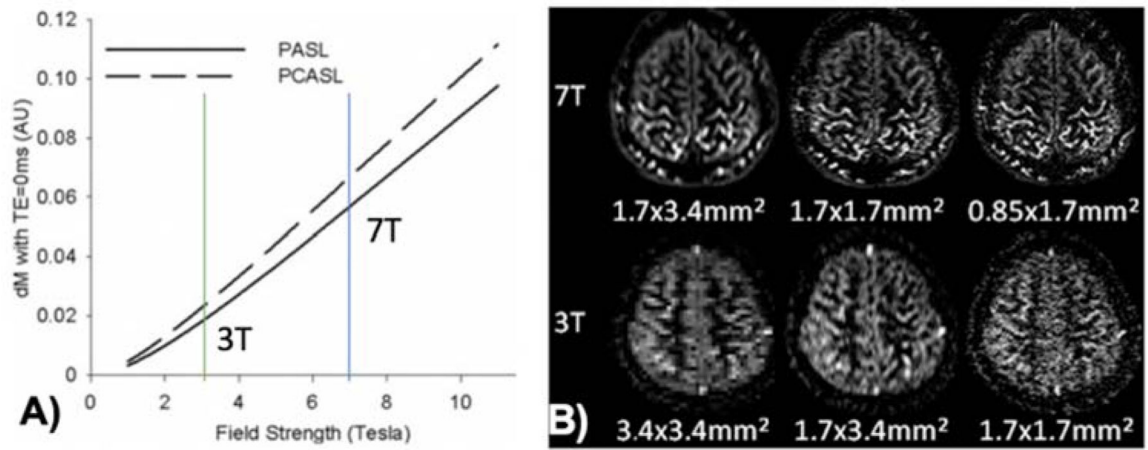
Figure 2.
(A) Theoretical calculation of PASL and pCASL signals as a function of field strength, showing >3-fold SNR gain from 3 to 7T. (B) pCASL perfusion images at 7T and 3T with 3 different resolutions. *Adapted from* Zuo Z, Wang R, Zhuo Y, et al. Turbo-FLASH based arterial spin labeled perfusion MRI at 7 T. PloS one. 2013;8(6). With permission.
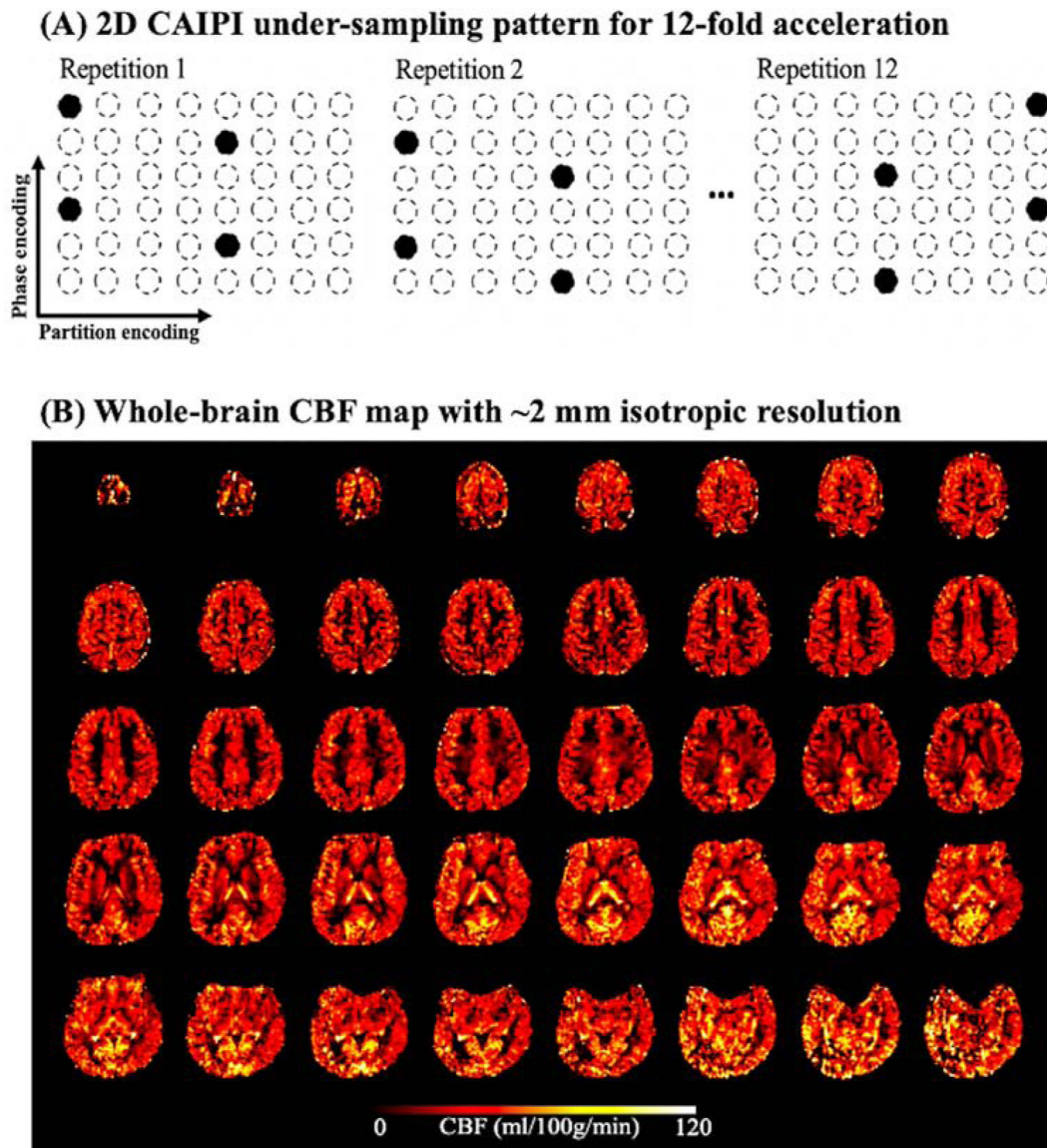
(A) 2D CAIPI under-sampling pattern for 12-fold acceleration

(B) Whole-brain CBF map with ~2 mm isotropic resolution

Figure 3.
(A) Implementation of the time-dependent 2D CAIPI under-sampling pattern. Acceleration factor is three along phase encoding direction and four along partition encoding direction. Total acceleration factor is twelve. Acceleration pattern is shifted between repetitions along phase/partition encoding direction to increase the temporal incoherence. (B) Whole brain CBF map acquired with 2D-CAIPI acquisition and spatial/temporal TGV reconstruction. *Adapted from* Shao X, Spann SM, Wang K, et al. High-resolution whole brain ASL perfusion imaging at 7T with 12-fold acceleration and spatial-temporal regularized reconstruction. Intl Soc Mag Reson Med. 2020;Vol 28. With permission.
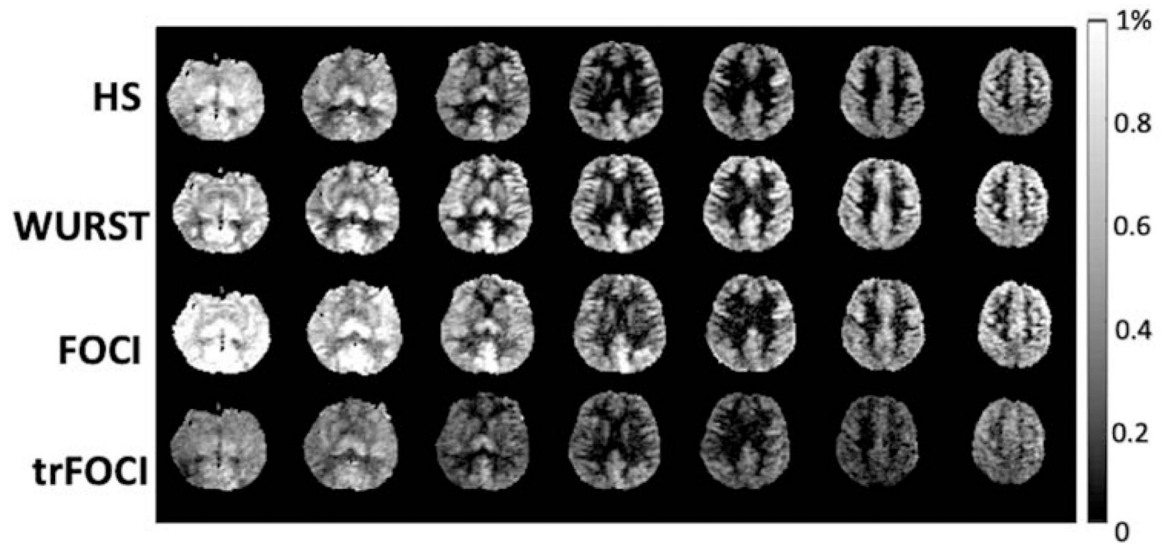
Figure 4.
Perfusion map acquired using the optimized adiabatic inversion pulses. For HS and FOCI, the residual tissue signal is dominant at bottom slices. the mean gray matter perfusion is 0.42%, 0.60%, 0.59%, 0.35%, for HS, WURST, FOCI and trFOCI, respectively. *Adapted from* Wang K, Shao X, Yan L, et al. Optimization of adiabatic pulses for Pulsed ASL at 7T – Comparison with Pseudo-continuous ASL. Proc ISMRM 2020;28:3695; with permission.
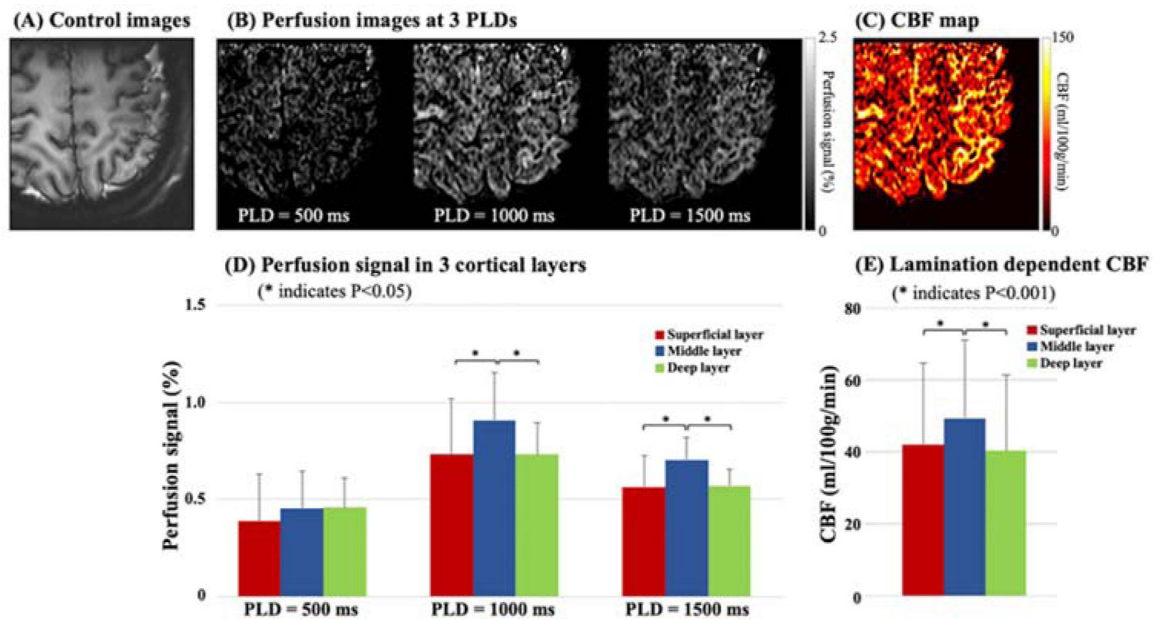
Figure 5.

Multi-delay perfusion images (B) and CBF maps (C) with sub-millimeter in-plane resolution (0.5 mm, after interpolation) acquired at 7T. (A) shows the corresponding structural control images. Small FOV was acquired using inner-volume 3D GRASE readout to shorten the acquisition time and increase SNR. (D) shows the bar plot of perfusion signal (normalized by M0) at PLD = 500, 1000, and 1500 ms in three layers of motor cortex. Multi-delay perfusion images reveal the dynamic passage of labeled signals, and the majority of labeled spins arrive into capillary space at PLD = 1000 ms. Perfusion signal in the middle layer is significantly higher (~20%) than the superficial or deep layer at PLD = 1000 and 1500 ms. (E) shows the bar plot of CBF, which was computed by a weighted-delay approach. CBF in the middle layer is 17.3% higher than the superficial layer and 22.7% higher than the deep layer.
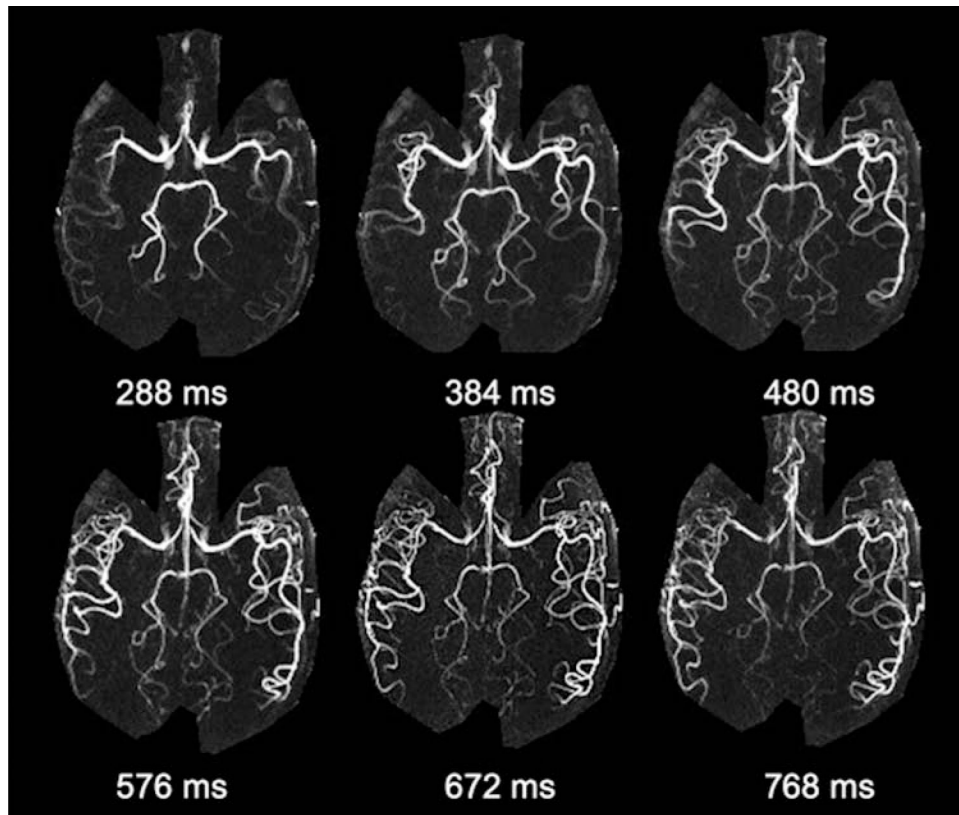
Figure 6.
An example of 4D MRA using 3D Cartesian acquisition with spatial resolution of 1×1×1 mm^3 at 7T. Six representative 4D MRA maximum intensity projection (MIP) images along the axial direction are displayed. Detailed delineation of dynamic blood flow through cerebral vasculature can be appreciated.
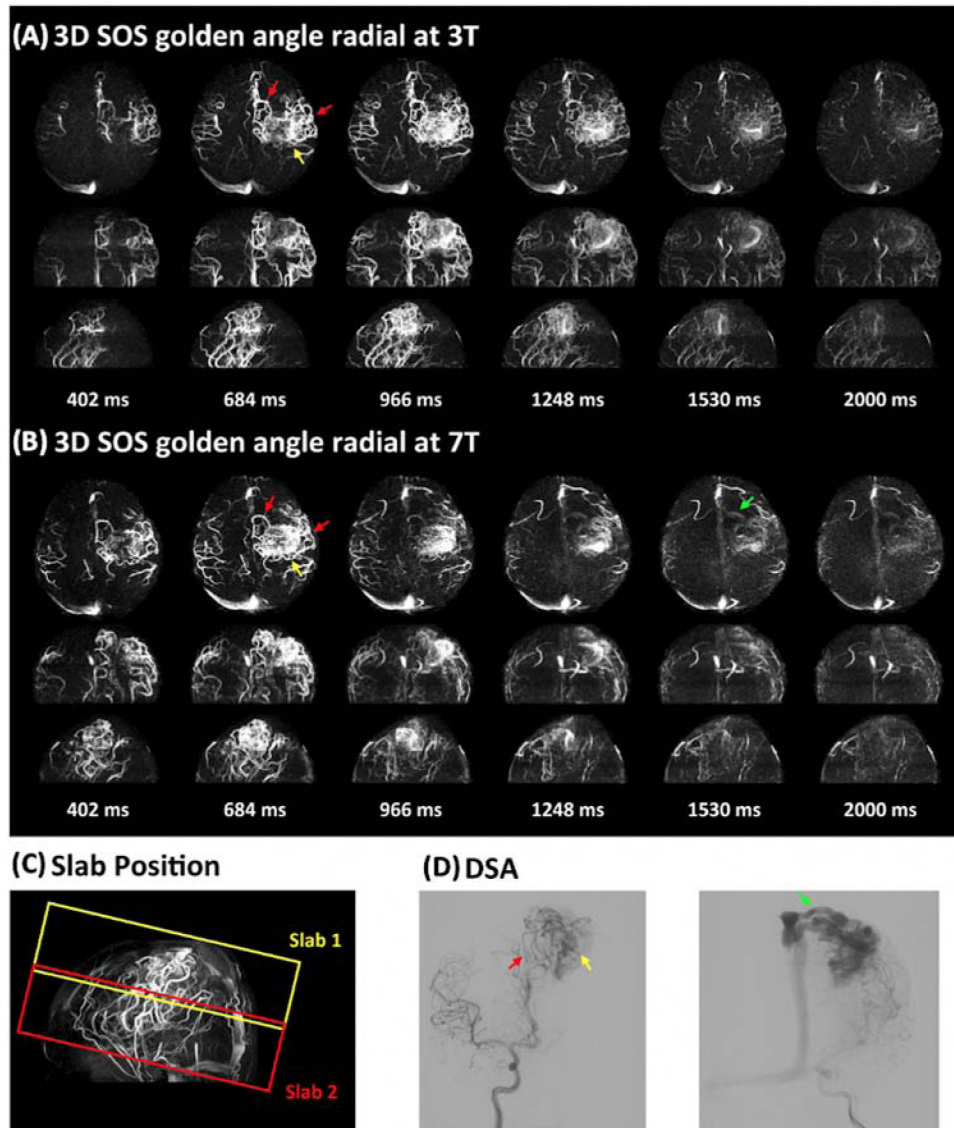
Figure 7.
An AVM case with two slabs acquired with 4D MRA using golden-angle stack-of-stars radial acquisition at 3T (A) and 7T (B). Six representative maximum intensity projection (MIP) images are displayed along axial, coronal, and sagittal views. The positions of the two slabs are shown in the TOF image (C). DSA images serve as the gold standard (D). The entire AVM lesion including feeding arteries (red arrow), nidus (yellow arrow), and draining vein (green arrow) was captured in a two-slab radial 4D MRA. 4D MRA matches well with DSA. It can be noted that the draining vein (green arrow in b) is better depicted at 7T than that at 3T. *Adapted from* Cong F, Zhuo Y, Yu S, et al. Noncontrast-enhanced time-resolved 4D dynamic intracranial MR angiography at 7T: A feasibility study. J Magn Reson Imaging. 2018;48(1):111–120; with permission.
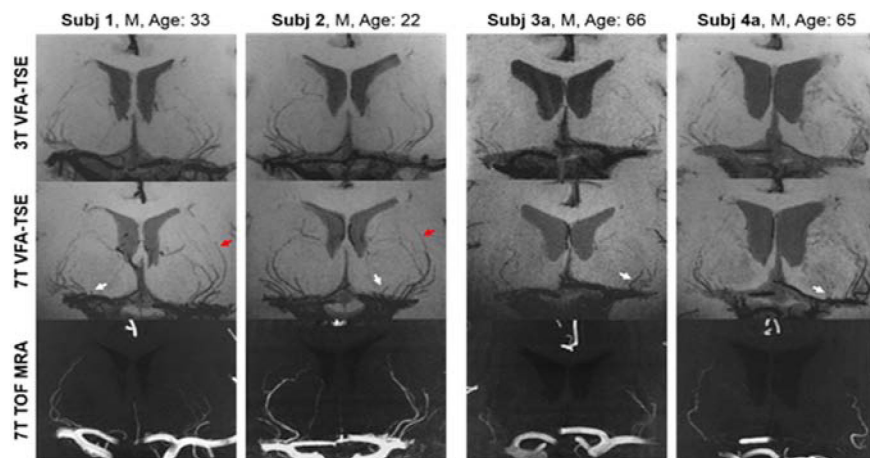
Figure 8.
Coronal 10 mm thin slice minimum intensity projections of both young and aged subject TSE-VFA scans at 3.0 Tesla (top row) and 7.0 Tesla (middle row). With the increased field strength, LSAs are more clearly delineated, especially in the distal portions of the vessels (red arrows). The bottom row shows coronal 10 mm thin slice maximum intensity projection of 7T TOF MRA. TSE-VFA can resolve more LSAs than 7T TOF MRA, especially for the LSAs located in the medial group along the middle cerebral artery (white arrows). *Adapted from* Ma SJ, Sarabi MS, Yan L, et al. Characterization of lenticulostriate arteries with high resolution black-blood T1-weighted turbo spin echo with variable flip angles at 3 and 7 Tesla. Neuroimage. 2019;199:184–193; with permission.
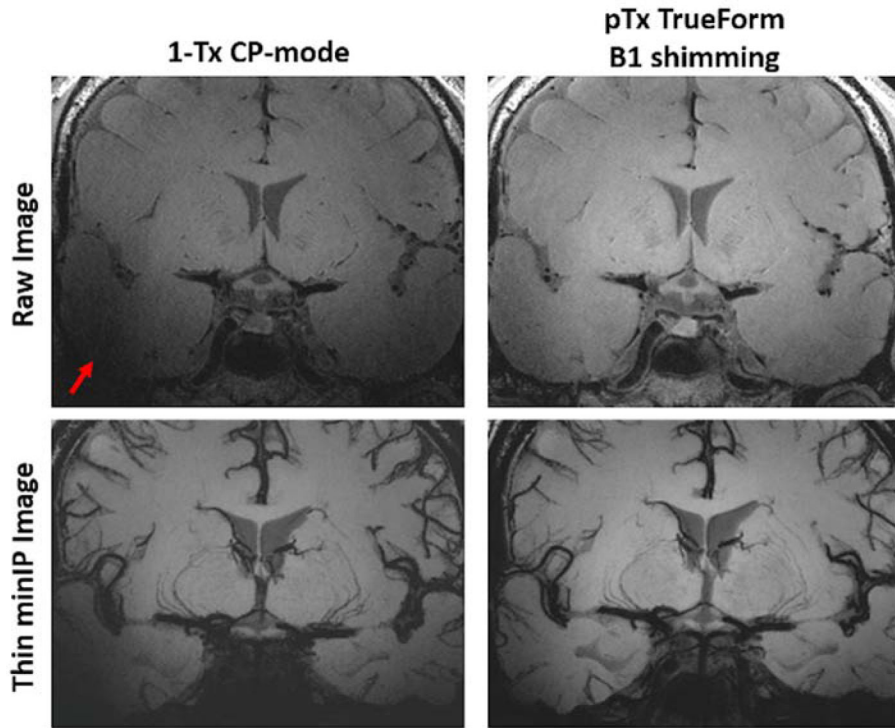
Figure 9.
The LSAs are located in the central "bright spot" of the B1+ field due to standing wave shading artifacts (dielectric effects, red arrow) at 7T, which is favorable for enhancing the CNR of LSAs but problematic for evaluating larger vessels at the base of the brain or perforating arteries in the parenchyma. With the use of pTx B1 shimming, the dielectric effects toward the base of the brain are reduced, improving overall SNR and enabling concurrent vessel wall assessment.